

Excitations of the unstable nuclei ^{48}Ni and ^{49}Ni

S. P. Kamedzhiev

Institute of Physics and Power Engineering, 249020 Obninsk, Russia

V. I. Tselyaev

Nuclear Physics Department, V. A. Fock Institute of Physics, St. Petersburg State University, 198504 St. Petersburg, Russia

(Received 29 July 2002; published 17 October 2002)

The isoscalar $E1$ and $E2$ resonances in the proton-rich nuclei $^{48,49}\text{Ni}$ and the $\{f_{7/2} \otimes 3^-\}$ multiplet in ^{49}Ni have been calculated taking into account the single-particle continuum exactly. The analogous calculations for the mirror nuclei ^{48}Ca and ^{49}Sc are presented. The models used are the continuum random-phase approximation (RPA) for ^{48}Ni , ^{48}Ca and the odd RPA for ^{49}Ni , ^{49}Sc , where the latter has been developed recently and describes both single particle and collective excitations of an odd nucleus on a common basis. In all four nuclei, we obtained a distinct splitting of the isoscalar $E1$ resonance into $1\hbar\omega$ and $3\hbar\omega$ peaks at about 11 MeV and 30 MeV, respectively. The main part of the isoscalar $E1$ energy-weighted sum rule (EWSR) is exhausted by the $3\hbar\omega$ resonances. The $1\hbar\omega$ resonances exhaust about 35% of this EWSR in $^{48,49}\text{Ni}$ and about 22% in ^{48}Ca and ^{49}Sc . All seven $\{f_{7/2} \otimes 3^-\}$ multiplet members in ^{49}Ni are calculated to be in the 6–8 MeV energy region and have noticeable escape widths.

DOI: 10.1103/PhysRevC.66.044304

PACS number(s): 21.60.Jz, 24.30.Cz, 27.40.+z

The main feature of the proton-rich unstable nuclei ^{48}Ni and ^{49}Ni , which have been discovered recently [1,2], is that they have a proton separation energy near zero. It seems to be of great interest to calculate excitations of these nuclei, especially in the framework of the same calculational scheme, which would take into account the single-particle continuum reliably because its role is obviously very important in this case, though the corresponding effects may not be so strong as in the neutron-rich nuclei with the neutron separation energy near zero. The comparison of the theoretical predictions with future measurements of the excitations of these nuclei will make it possible to obtain an important information about the nucleon-nucleon effective interaction in drip-line nuclei and about features of such nuclei, which are also of astrophysical interest.

For the doubly magic ^{48}Ni , one of the proper microscopic methods is the theory of finite Fermi systems (TFFS) [3] with exact accounting for the single-particle continuum (continuum TFFS). It corresponds to the continuum random-phase approximation (RPA) making use of the phenomenological Landau-Migdal particle-hole (p - h) interaction and a single-particle Woods-Saxon scheme. The parameters describing this interaction and the single-particle scheme are known [4–6], at least for stable nuclei, and it is of great interest to check them for unstable ones.

For doubly magic nuclei plus or minus one nucleon, a theory has been developed recently [7], which was termed the odd RPA (ORPA). It corresponds to the continuum RPA for even-even nuclei and, in addition, consistently accounts for properties of odd nuclei. The ORPA allows a consistent description of both the single particle and collective part of the excitation spectrum of an odd nucleus without pairing, including giant resonances in the continuum and splitting of particle (hole) \otimes phonon multiplets, on a common basis. The description of these multiplets taking the single-particle continuum into account is especially important and interesting for nuclei such as ^{49}Ni with the nucleon separation energy

near zero and relatively large phonon energies. Other questions concerning the excitations of this nucleus exist. For example, it was shown in Ref. [7] that the isoscalar (IS) $E1$ strength in ^{17}O below 12.5 MeV is completely determined by the odd nucleon contribution. The question about a similar effect in ^{49}Ni arises.

Thus, we have a reasonable and a very interesting possibility to calculate excitations of both nuclei within the same calculational scheme based on the continuum TFFS as well as to investigate primarily the role of the small proton separation energy in the proton-rich $^{48,49}\text{Ni}$ nuclei and of the single-particle continuum. This is the aim of the present paper. We will present the results of the calculations of the IS $E1$ and $E2$ giant resonances in ^{48}Ni and ^{49}Ni . For ^{49}Ni , the characteristics of the $\{f_{7/2} \otimes 3^-\}$ multiplet will be presented for all seven resonances. For comparison and reliability of the results, the resonances in the mirror nuclei ^{48}Ca , ^{49}Sc and the multiplet in ^{49}Sc are also calculated. In the calculations we use the TFFS and Woods-Saxon potential parameters which are mainly known. However, in order to have reliable results for the exotic nuclei, we fit some of the parameters of the Landau-Migdal interaction and Woods-Saxon potential using Hartree-Fock single-particle levels obtained with the known Skyrme interaction and experimental data for ^{48}Ca nucleus (see below).

In the TFFS approach [3], the effective interaction and the single-particle scheme are described by two sets of phenomenological parameters and are not connected with each other. In our calculations the single-particle potential was taken in the form

$$U_q(\mathbf{r}) = U_q^0 f_{WS}(r) + U_q^{so} \frac{\kappa}{r} \frac{df_{WS}(r)}{dr} (\mathbf{1} \cdot \boldsymbol{\sigma}) + U_C(r), \quad (1)$$

where $f_{WS}(r) = 1/(1 + \exp[(r-R)/a])$, index $q = n, p$ denotes the sort of the nucleon. The Coulomb potential U_C for pro-

tons is that of a uniformly charged sphere. The parameters U_q^{so} , κ , R , and a used here are well known [6],

$$\begin{aligned} U_p^{so} &= (ZV_{pp} + NV_{pn})/A, & U_n^{so} &= (NV_{nn} + ZV_{np})/A, \\ V_{pp} &= V_{nn} = 19.7 \text{ MeV}, & V_{pn} &= V_{np} = 87.0 \text{ MeV}, \\ \kappa &= 0.263[1 + 2(N-Z)/A] \text{ fm}^2, \\ R &= 1.24A^{1/3} \text{ fm}, & a &= 0.63 \text{ fm}. \end{aligned}$$

The choice of the parameters U_q^0 in Eq. (1) is a more complicated question for the $^{48,49}\text{Ni}$ nuclei. The point is that the value of U_p^0 cannot be determined from the standard set of parameters [6], which corresponds to $U_q^0 = U_q^{so}$ in Eq. (1), because in this case it leads to a positive energy of the last occupied proton $1f_{7/2}$ level in ^{48}Ni . To overcome this difficulty we used the following method. We have calculated the energies of single-particle proton and neutron $1f_{7/2}$ levels in ^{48}Ni in the framework of the self-consistent Hartree-Fock method with the Skyrme SIII interaction of Ref. [8], which is often used in the calculations of properties of both stable and unstable nuclei. Then the values of the potential depths U_p^0 and U_n^0 in Eq. (1) were fitted so as to reproduce the Hartree-Fock values of $\varepsilon_p(1f_{7/2}) = -0.86 \text{ MeV}$ and $\varepsilon_n(1f_{7/2}) = -16.98 \text{ MeV}$. From this input we obtained $U_p^0 = -52.03 \text{ MeV}$, $U_n^0 = -60.98 \text{ MeV}$ for ^{48}Ni . The same procedure was performed for the ^{48}Ca nucleus. In this case the values $U_p^0 = -58.32 \text{ MeV}$ and $U_n^0 = -49.09 \text{ MeV}$ yield the Hartree-Fock values of the single-particle energies $\varepsilon_p(1f_{7/2}) = -10.16 \text{ MeV}$ and $\varepsilon_n(1f_{7/2}) = -9.99 \text{ MeV}$. The corresponding experimental values for ^{48}Ca are -9.63 MeV and -9.95 MeV , i.e., the agreement with experiment is fairly good.

The Landau-Migdal p - h interaction used in our calculation is defined by the following ansatz:

$$\begin{aligned} \mathcal{F}(\mathbf{r}_1, \mathbf{r}_2) &= C_0[f(\mathbf{r}_1) + f'(\mathbf{r}_1)(\boldsymbol{\tau}_1 \cdot \boldsymbol{\tau}_2) + g(\boldsymbol{\sigma}_1 \cdot \boldsymbol{\sigma}_2) \\ &+ g'(\boldsymbol{\tau}_1 \cdot \boldsymbol{\tau}_2)(\boldsymbol{\sigma}_1 \cdot \boldsymbol{\sigma}_2)]\delta(\mathbf{r}_1 - \mathbf{r}_2), \end{aligned} \quad (2)$$

where

$$\begin{aligned} f(\mathbf{r}) &= f_{ex} + (f_{in} - f_{ex})\rho(\mathbf{r})/\rho(0), \\ f'(\mathbf{r}) &= f'_{ex} + (f'_{in} - f'_{ex})\rho(\mathbf{r})/\rho(0). \end{aligned} \quad (3)$$

The total nucleon density $\rho(\mathbf{r})$ entering Eq. (3) is defined in our approach by the formula

$$\rho(\mathbf{r}) = \sum_{\lambda, \sigma} n_\lambda |\varphi_\lambda(\mathbf{r}, \sigma)|^2, \quad (4)$$

where n_λ are the occupation numbers, φ_λ are the single-particle wave functions calculated within the above-described Woods-Saxon scheme.

The parameters entering Eq. (2) are known [4,5], as a rule, except for one of the six parameters, namely, the parameter f_{ex} , which is fitted very often to the experimental energies of low-lying phonons, see, for example, Refs. [7,9].

In our case this is especially necessary because, strictly speaking, there is no guarantee that the Landau-Migdal interaction is suitable for the drip-line nuclei. Since the excitations of ^{48}Ni are unknown, it is reasonable to use known excitations of the mirror nucleus ^{48}Ca for adjusting f_{ex} . So we have fitted the parameter f_{ex} to reproduce (within the continuum TFFS) the energy of the 3_1^- level in ^{48}Ca at 4.51 MeV. The result was $f_{ex} = -0.94$. Thus, in all our calculations the following set of the Landau-Migdal interaction parameters has been used (the rest of them being taken from Refs. [4,5,7,9]):

$$\begin{aligned} f_{ex} &= -0.94, & f_{in} &= -0.002, & f'_{ex} &= 2.30, & f'_{in} &= 0.76, \\ g &= 0.05, & g' &= 0.96, & C_0 &= 300 \text{ MeV fm}^3. \end{aligned}$$

With these parameters we obtained a reasonable agreement with experiment for 2_1^+ level [$E_{th}(2_1^+) = 4.15 \text{ MeV}$, $E_{exp}(2_1^+) = 3.83 \text{ MeV}$] and very good agreement for the $B(E3)\uparrow = B(E3, \text{g.s.} \rightarrow 3_1^-)$ value [$B_{th}(E3)\uparrow = 6500 \text{ e}^2 \text{ fm}^6$ and $B_{exp}(E3)\uparrow = 6700 \text{ e}^2 \text{ fm}^6$] in ^{48}Ca . The latter is important for the realistic description of the $\{f_{7/2} \otimes 3^-\}$ multiplet.

The calculations of the IS $E1$ and $E2$ resonances in ^{48}Ni and ^{48}Ca were performed within continuum TFFS. For the IS $E1$ resonance, the ‘‘forced consistency’’ and the spurious state suppression procedure was applied. This procedure and other details of the calculational scheme have been described in Refs. [7,10]. The same resonances and the $\{f_{7/2} \otimes 3^-\}$ multiplets in ^{49}Ni and ^{49}Sc have been calculated within the ORPA model developed in Ref. [7]. In the ORPA calculations, only one (entrance) channel was incorporated and same interaction parameters and the single-particle schemes were used as in our TFFS ones. All the calculations were performed using the coordinate representation technique in the framework of the Green function method [11] which enables one to take into account the single-particle continuum exactly. The smearing parameters used were $\Delta = 300 \text{ keV}$ for the giant resonances and $\Delta = 0.2 \text{ keV}$ for the multiplets.

One-body transition operators (i.e., the external field operators V^0 in terms of TFFS) were taken in the following form:

$$V_q^{0(E1)} = (r^3 - R_{IS}^2 r) Y_{1\mu}(\hat{r}) \quad (5)$$

for isoscalar $E1$ excitations,

$$V_q^{0(E2)} = r^2 Y_{2\mu}(\hat{r}) \quad (6)$$

for isoscalar $E2$ excitations, and

$$V_q^{0(E3)} = e_q r^3 Y_{3\mu}(\hat{r}) \quad (7)$$

for electromagnetic $E3$ excitations, where e_q are the nucleon effective charges in the center-of-mass reference frame (see, e.g., Ref. [11]):

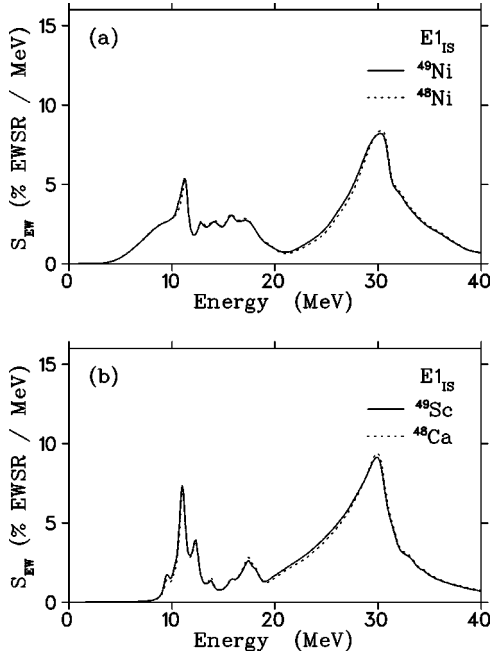


FIG. 1. The normalized energy-weighted strength functions $S_{EW}(E)$ for the isoscalar (IS) $E1$ excitations in ^{49}Ni (a) and ^{49}Sc (b) calculated in the ORPA (solid lines), and the same functions for ^{48}Ni (a) and ^{48}Ca (b) calculated in the continuum TFFS (dotted lines). The smearing parameter is $\Delta = 300$ keV.

$$e_p = \left[\left(1 - \frac{1}{A} \right)^L + (Z-1) \left(-\frac{1}{A} \right)^L \right] e, \quad e_n = Z \left(-\frac{1}{A} \right)^L e, \quad (8)$$

with $L=3$. Parameter R_{IS} in Eq. (5) is determined within the “forced consistency” scheme (see, Ref. [7]). In the present calculations the numerical values of R_{IS} for all nuclei under consideration are very close (within 1%) to those of $(\frac{5}{3}\langle r^2 \rangle)^{1/2}$ (in this context, see Ref. [12]).

The results for the IS $E1$ and $E2$ resonances are presented in Figs. 1 and 2 in the form of the normalized energy-weighted strength functions $S_{EW}(E)$:

$$S_{EW}(E) = \frac{100}{m_1^{SR}} E S(E), \quad (9)$$

where $S(E)$ is the RPA (ORPA) strength function, m_1^{SR} is the corresponding energy-weighted sum rule (EWSR), which is defined as

$$m_1^{SR} = \frac{3\hbar^2 A}{8m\pi} \left(11\langle r^4 \rangle - \frac{25}{3}\langle r^2 \rangle^2 \right) \quad (10)$$

for the IS $E1$ operator (5), and

$$m_1^{SR} = \frac{25\hbar^2 A}{4m\pi} \langle r^2 \rangle \quad (11)$$

for the IS $E2$ operator (6). Note that these formulas differ from the often used definitions of the IS EL EWSR (see, Refs. [12,13]) by the factor $(2L+1)$ arising due to the sum-

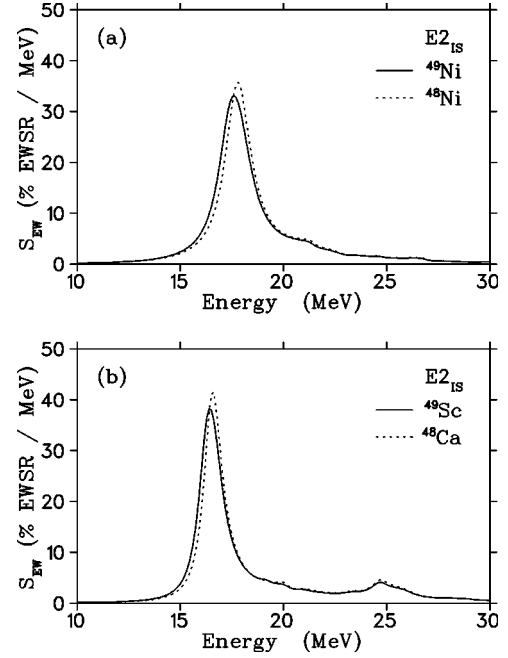


FIG. 2. Same as Fig. 1, but for the isoscalar $E2$ resonance.

mation over the quantum numbers of the excited states and of an external field in the strength functions.

The functions $S_{EW}(E)$ for IS $E1$ excitations of all the nuclei considered are shown in Fig. 1. The IS $E1$ strength is distributed around two main maxima at about 11 MeV and 30 MeV, which correspond to the $1\hbar\omega$ and $3\hbar\omega$ IS $E1$ resonances. The calculated position of the $3\hbar\omega$ resonances is in agreement with the experimental formula $E_x \sim 114A^{-1/3} = 31.4$ MeV for $A=48$, which was obtained in Ref. [14] for the upper components of the IS $E1$ resonances in ^{90}Zr , ^{116}Sn , and ^{208}Pb . To estimate the contribution of these resonances into the IS $E1$ EWSR (10) the following integrals were calculated:

$$p(E_{min}; E_{max}) = \int_{E_{min}}^{E_{max}} S_{EW}(E) dE. \quad (12)$$

The contribution of the $1\hbar\omega$ resonance [$p(1\hbar\omega)$] was defined as $p(0;21)$ in ^{48}Ni , ^{49}Ni (hereinafter the values of E_{min} and E_{max} are given in MeV), and as $p(0;19)$ in ^{48}Ca , ^{49}Sc , where the values of 21 MeV and 19 MeV are the energies of minima separating $1\hbar\omega$ and $3\hbar\omega$ resonances in these nuclei. For the $3\hbar\omega$ resonance the contribution [$p(3\hbar\omega)$] was defined as $p(21;40)$ in ^{48}Ni , ^{49}Ni , and as $p(19;40)$ in ^{48}Ca , ^{49}Sc . The results, which are listed in Table I, show that the main part of the IS $E1$ EWSR is exhausted by the $3\hbar\omega$

TABLE I. The percentages of the IS $E1$ EWSR for the $1\hbar\omega$ and $3\hbar\omega$ IS $E1$ resonances (see text for details).

% EWSR	^{48}Ni	^{49}Ni	^{48}Ca	^{49}Sc
$p(1\hbar\omega)$	35	35	21	22
$p(3\hbar\omega)$	59	60	73	73

TABLE II. Energy of the maximum E_0 , the width at half maximum Γ_0 , and the percentage of the IS $E2$ EWSR in the energy interval 10–30 MeV for IS GQR.

	^{48}Ni	^{49}Ni	^{48}Ca	^{49}Sc
E_0 (MeV)	17.8	17.6	16.6	16.4
Γ_0 (MeV)	1.5	1.8	1.1	1.3
p (IS GQR), % EWSR	94	94	91	92

resonances in all nuclei under consideration. The $1\hbar\omega$ resonance exhausts about 35% of the IS $E1$ EWSR in $^{48,49}\text{Ni}$ and about 22% in ^{48}Ca and ^{49}Sc .

Further, comparing the results for the doubly magic and neighboring odd nuclei in Fig. 1, we see that the role of the odd nucleon is rather small in our case. The difference from the IS $E1$ resonances in ^{16}O and ^{17}O (see Ref. [7]) is that in ^{49}Ni and ^{49}Sc the single-particle resonances are embedded into the region of the core p - h excitations and are only slightly distinguishable against their background.

The IS $E2$ resonances in ^{48}Ni , ^{49}Ni , ^{48}Ca , and ^{49}Sc are shown in Fig. 2. Their characteristics are given in Table II. We obtained a reasonable depletion of the IS $E2$ EWSR within the 10–30 MeV interval taken. The positions of the maxima of the calculated strength functions are in a reasonable agreement with an empirical formula for the mean energy of the IS giant quadrupole resonance (GQR) $\bar{E}_{IS\ GQR} \sim 63A^{-1/3}$ MeV = 17.3 MeV for $A=48$ and with the mean energy $\bar{E} = 16.9$ MeV obtained for ^{48}Ca in Ref. [15] in the $1p1h + 1p1h \otimes \text{phonon} + \text{GSC}_{\text{phonon}}$ approximation. The

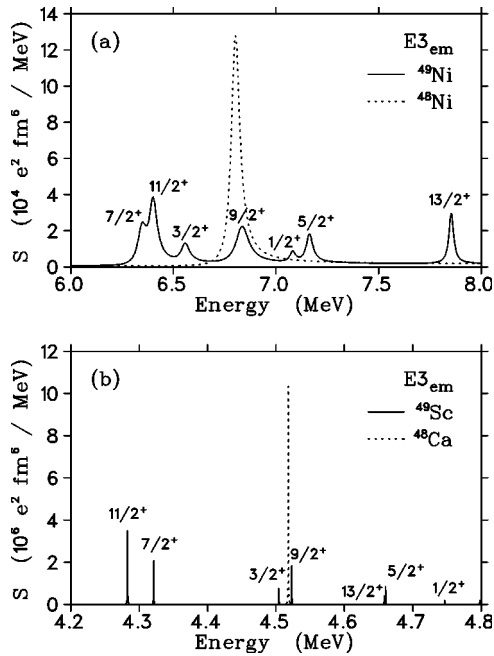


FIG. 3. The electromagnetic $E3$ strength functions $S(E)$ for ^{49}Ni (a) and ^{49}Sc (b) calculated in the ORPA (solid lines), and the same functions for ^{48}Ni (a) and ^{48}Ca (b) calculated in the continuum TFES (dotted lines). The smearing parameter is $\Delta = 0.2$ keV.

TABLE III. Characteristics of the septuplet members $\{f_{7/2} \otimes 3_1^-\}_{j^\pi}$ in ^{49}Ni and ^{49}Sc . The calculated energy shifts δE from the excitation energies of 3_1^- states in ^{48}Ni [$E(3_1^-) = 6.802$ MeV] and ^{48}Ca [$E(3_1^-) = 4.518$ MeV] are shown. The escape widths Γ^\uparrow for the septuplet members in ^{49}Ni are given. The values of $B(E3, j^\pi \rightarrow \text{g.s.})$ are shown in Weisskopf units (1 W.u. = $142.6 e^2 \text{ fm}^6$).

j^π	^{49}Ni			^{49}Sc	
	δE (keV)	Γ^\uparrow (keV)	$B(E3)$ (W.u.)	δE (keV)	$B(E3)$ (W.u.)
$\frac{1}{2}^+$	279	33	11.1	228	3.4
$\frac{3}{2}^+$	-244	49	13.9	-14	6.7
$\frac{5}{2}^+$	361	39	11.4	142	5.1
$\frac{7}{2}^+$	-455	52	14.7	-197	10.1
$\frac{9}{2}^+$	33	77	16.2	5	6.9
$\frac{11}{2}^+$	-401	46	14.3	-235	10.3
$\frac{13}{2}^+$	1052	28	6.7	140	1.0

present results for IS GQR in ^{48}Ca are also in good agreement with those obtained in Refs. [16,17] within the self-consistent continuum RPA [in Ref. [16], the maximum of $S(E)$ was obtained at 16.6 MeV, and 87% of the IS $E2$ EWSR was found within the 14–19 MeV interval]. However, in our calculation the peak energy of IS GQR in ^{48}Ni is about 1.8 MeV shifted upwards from the value of 16.0 MeV obtained in Ref. [17]. This considerable discrepancy seems to be explained by the difference between the single-particle schemes and between the effective forces used in the calculations being compared. The case of the ^{48}Ni nucleus appears to be more sensitive to this difference due to the small proton separation energy.

From comparison of the results presented in Figs. 1 and 2, one can see that the proximity of the proton separation energy to zero in $^{48,49}\text{Ni}$ is especially manifested in the case of $1\hbar\omega$ IS $E1$ resonance giving rise to a noticeable increase of its escape width Γ^\uparrow and to the larger depletion of the IS EWSR (about 35%) as compared with ^{48}Ca and ^{49}Sc (about 22%). The broadening of the IS $E2$ resonances in the unstable nuclei can also be seen from the results presented in Table II.

Note, however, that our calculations cannot pretend to describe total width of the resonances because only two main damping mechanisms (Landau and escape ones) were taken into account while the third one, i.e., the spreading-width formation mechanism, was not included in the calculations (for such kind of calculations in ^{48}Ca , see, Ref. [15]).

At last but not the least, in Fig. 3 we show the strength functions for the $\{f_{7/2} \otimes 3_1^-\}$ multiplets in ^{49}Ni and ^{49}Sc together with the 3_1^- levels in ^{48}Ni and ^{48}Ca , respectively. Here the neutron $1f_{7/2}$ single-particle level corresponds to the ground state (g.s.) of the ^{49}Ni nucleus, the proton $1f_{7/2}$ level corresponds to the g.s. of the ^{49}Sc . As compared with the giant resonances (Figs. 1 and 2) we see a very natural and noticeable role of the odd neutron in ^{49}Ni and proton in ^{49}Sc . All seven multiplet members are around the 3_1^- level

of the core at 6.8 MeV in the case of ^{49}Ni and at 4.5 MeV in the case of ^{49}Sc . Since the 3_1^- level in ^{48}Ni lies in the continuum (and consequently is a resonance), each of the multiplet members in ^{49}Ni has a noticeable escape width Γ^\dagger . Our approach enables one to calculate the escape width immediately because the single-particle continuum is included completely. The value of Γ^\dagger was determined as a width at half maximum of the corresponding strength function (note that the smearing parameter $\Delta = 0.2$ keV in Fig. 3). The calculated value for ^{48}Ni is $\Gamma^\dagger(3_1^-) = 51$ keV. For the multiplets members, the values of Γ^\dagger , energy shifts δE , and $B(E3, j^\pi \rightarrow \text{g.s.})$ are listed in Table III. It is of great interest to measure the resonances in ^{49}Ni and their “pure” escape widths, which may be an easier task at present than the measurement of the 3_1^- level in ^{48}Ni .

In conclusion, we have calculated some excitations in ^{48}Ni , ^{49}Ni , ^{48}Ca , and ^{49}Sc within the same calculational

scheme and with the consistent account for the single-particle continuum. Despite the fact that more complex configurations have not been accounted for in the calculations, our results expected to be realistic enough to be compared with experiment. In all four nuclei considered, a distinct splitting of the IS $E1$ resonance into two peaks at about 11 MeV and 30 MeV has been obtained. The influence of the small proton separation energy in $^{48,49}\text{Ni}$ has been demonstrated, especially on the escape width and a large depletion of the IS $E1$ EWSR by the $1\hbar\omega$ IS $E1$ resonance. For the $\{f_{7/2} \otimes 3^-\}$ multiplet in ^{49}Ni , the widths of all the multiplet members are formed by the single-particle continuum in our approach. Measurements of these excitations, including escape widths of the individual states, will give valuable information about many features of drip-line nuclei.

The authors are very grateful to Professor V. R. Brown for her advice and careful reading of the manuscript.

-
- [1] B. Blank, S. Czajkowski, F. Davi, R. Del Moral, J.P. Dufour, A. Fleury, C. Marchand, M.S. Pravikoff, J. Benlliure, F. Boué, R. Collatz, A. Heinz, M. Hellström, Z. Hu, E. Roeckl, M. Shibata, K. Sümmerer, Z. Janas, M. Karny, M. Pfützner, and M. Lewitowicz, Phys. Rev. Lett. **77**, 2893 (1996).
- [2] B. Blank, M. Chartier, S. Czajkowski, J. Giovinazzo, M.S. Pravikoff, J.-C. Thomas, G. de France, F. de Oliveira Santos, M. Lewitowicz, C. Borcea, R. Grzywacz, Z. Janas, and M. Pfützner, Phys. Rev. Lett. **84**, 1116 (2000).
- [3] A. B. Migdal, *Theory of Finite Fermi Systems and Applications to Atomic Nuclei* (Interscience, New York, 1967), (Nauka, Moscow, 1983) (in Russian).
- [4] A.V. Smirnov, S.V. Tolokonnikov, and S.A. Fayans, Yad. Fiz. **48**, 1661 (1988) [Sov. J. Nucl. Phys. **48**, 995 (1988)].
- [5] I.N. Borzov, S.V. Tolokonnikov, and S.A. Fayans, Yad. Fiz. **40**, 1151 (1984) [Sov. J. Nucl. Phys. **40**, 732 (1984)].
- [6] V.A. Chepurinov, Yad. Fiz. **6**, 955 (1965) [Sov. J. Nucl. Phys. **6**, 696 (1967)].
- [7] S.P. Kamerzhiev, R.J. Liotta, and V.I. Tselyaev, Phys. Rev. C **63**, 034304 (2001).
- [8] M. Beiner, H. Flocard, Nguyen Van Giai, and P. Quentin, Nucl. Phys. **A238**, 29 (1975).
- [9] S.P. Kamerzhiev, G.Ya. Tertychny, and V.I. Tselyaev, Fiz. Elem. Chastits At. Yadra **28**, 333 (1997) [Phys. Part. Nucl. **28**, 134 (1997)].
- [10] S. Kamerzhiev, R.J. Liotta, E. Litvinova, and V. Tselyaev, Phys. Rev. C **58**, 172 (1998).
- [11] S. Shlomo and G. Bertsch, Nucl. Phys. **A243**, 507 (1975).
- [12] N. Van Giai and H. Sagawa, Nucl. Phys. **A371**, 1 (1981).
- [13] K.F. Liu and G.E. Brown, Nucl. Phys. **A265**, 385 (1976).
- [14] H.L. Clark, Y.-W. Lui, and D.H. Youngblood, Phys. Rev. C **63**, 031301(R) (2001).
- [15] S. Kamerzhiev, J. Speth, and G. Tertychny, Nucl. Phys. **A624**, 328 (1997).
- [16] I. Hamamoto, H. Sagawa, and X.Z. Zhang, Phys. Rev. C **55**, 2361 (1997).
- [17] I. Hamamoto, H. Sagawa, and X.Z. Zhang, Nucl. Phys. **A626**, 669 (1997).